Preparation, Structure Determination and Cytotoxicity of the Pd^{II}·Bleomycin A2 Complex

Athanasios Papakyriakou,[a] Ioannis Bratsos,[a] Maria Katsarou,[a] and Nikos Katsaros*[a]

Keywords: Bleomycin / Palladium / Molecular modelling / Cytotoxicity

The solution structure of the Pd^{II}·bleomycin A2 complex was resolved by NMR spectroscopy in combination with molecular modelling. The preparation of the complex in 1.0 M NaCl aqueous solutions leads to the formation of a major compound, which is very stable at ambient temperature. Our NMR spectroscopic data demonstrate that bleomycin is coordinated through the β-aminoalanine secondary amine, the pyrimidine ring N1, the deprotonated histidyl amide and the imidazole N1, in contrast to an earlier study that proposed coordination of the valerate amide. 2D NMR spectroscopic data were used as distance constraints in simulated annealing molecular-dynamics calculations and the first solution structure of a square-planar metallo-bleomycin is reported. In order to assess the toxicity of Pd^{II}·bleomycin, cytotoxicity measurements were performed in U937 and K562 leukemia cell lines using two methods. In both cell lines the free drug and the complex exhibit similar toxicity as a function of time.

Introduction

Bleomycins are a group of antibiotics with clinical use as anticancer drugs.[1−3] The commercial preparation, Bleocin or Blenoxane, consists predominantly of bleomycins A2 and B2 (Scheme 1). Their efficacy is mainly attributed to their ability to mediate cleavage of the DNA backbone by attacking at the deoxyribose 4′-H position and causing single- and double-strand cleavage and base release.[4−8] A number of putative pathways have been proposed to initiate DNA oxidation.[10,11] The drug is activated in the presence of iron and oxygen species as cofactors. Other metals can also facilitate DNA cleavage by bleomycin in vitro, even though their reactions are less well characterized.[12]

Umezawa and co-workers were the first to isolate bleomycins from the culture medium of *Streptomyces verticillus* and to propose the most likely metal-binding sites.[13] The X-ray crystal structure of Cu^{II}·P3A,[14,15] a biosynthetic intermediate of bleomycins lacking the linker, C-terminus and carbohydrate domains, revealed a five-coordinate square-pyramidal complex with five nitrogen donors. Only recently, Suguiyama et al.[16] obtained the X-ray crystal structures of both apo and Cu^{II}·bleomycin A2 bound with a protein and established the proposed metal-binding mode. The equatorial plane comprises the secondary amine of aminoalanine, the pyrimidine N1, the histidine amide and the imidazole N1, while the aminoalanine primary amine occupies the apical position (see Scheme 1). These structures were found to be consistent with the NMR models proposed by Stubbe et al. for the two Co^{III}·bleomycin adducts.[17−19] Among them, HO_2·Co^{III}·bleomycin is considered to be a robust structural analogue of the biologically relevant Fe·bleomycin.[20,21] Although Ga^{III} and In^{III}·bleomycins are not able to mediate DNA degradation, their solution structures were recently shown to bear strong resemblance to these models.[22,23] On the other hand, structural NMR studies on iron species have been carried out for the low-spin CO·Fe^{II}·bleomycin [24] and the paramagnetic Fe^{II}·bleomycin,[25] which exhibited contradictory results. Other direct structural studies on metallo-bleomycins have been performed with manganese,[26−28] ruthenium,[29,30] vanadyl,[31,32] zinc,[33−36] cadmium,[37] nickel,[38,39] calcium and trivalent lanthanides,[40] as well as the paramagnetic Co^{II}·bleomycin complex.[41,42]

In view of the fact that bleomycins are often administered in combination with cisplatin [*cis*-$PtCl_2(NH_3)_2$] for the treatment of malignant tumors,[43] Garnier-Suillerot and Albertini have carried out an investigation on the interaction between the two compounds.[44] Apart from cisplatin, *cis*-$PdCl_2(NH_3)_2$, $PdCl_2$(ethylenediamine) and $PdCl_4^{2-}$ were also used in this study. The final species, resulting from the interaction of these compounds with bleomycin, were suggested to be similar, albeit different reaction rates and formation constants were observed. Spectroscopic and potentiometric data have led the authors to propose a binding mode, which differs from the equatorial plane of most metallo-bleomycins. Instead of the imidazole ring N1, the valerate peptide nitrogen was proposed to be a donor atom of bleomycin, independent of the starting complex.

[a] Institute of Physical Chemistry, NCSR "Demokritos", 153 10 Ag. Paraskevi Attikis, Greece
Fax: (internat.) + 30-210-6511766
E-mail: katsaros@chem.demokritos.gr
Supporting information for this article is available on the WWW under http://www.eurjic.org or from the author.

  DOI: 10.1002/ejic.200400034

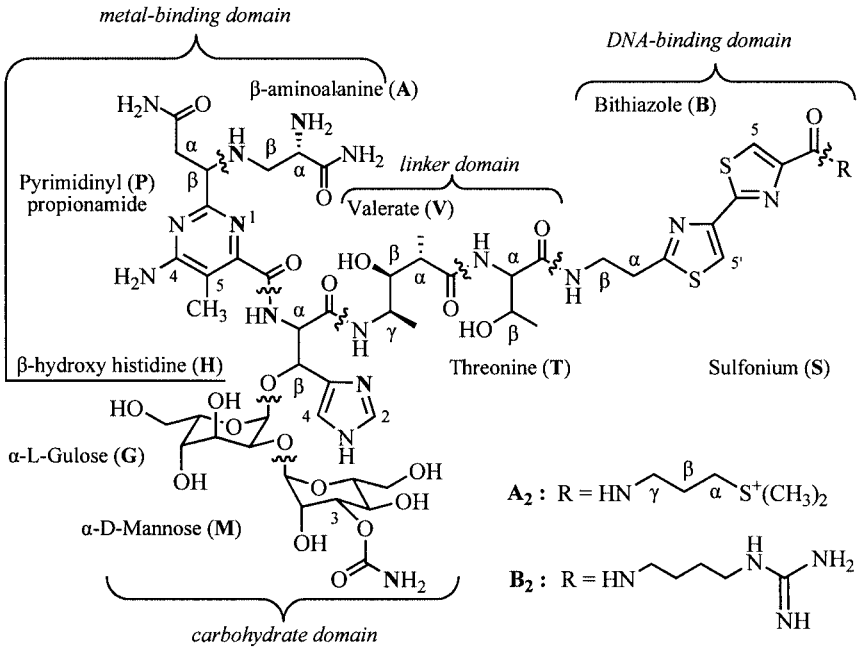

Scheme 1. Structure of bleomycins A2 and B2; the functional groups are separated by wavy lines and the potential N ligands are marked in bold

We have undertaken the preparation and structural characterization of Pd^{II}·bleomycin A2 with the aim to obtain its detailed solution structure through a combined use of NMR spectroscopy and molecular modelling. Our NMR spectroscopic data indicate that bleomycin binds strongly to Pd^{II} and forms a 1:1 adduct through four nitrogen donors, which comprise the equatorial plane of nearly all metallobleomycins. The combination of proton−proton distance constraints obtained by 2D NOESY experiments at low temperature, along with a suitable molecular mechanics force field for the modelling of Pd^{II}·bleomycin A2, have been used in determining its solution structure. Since no cytotoxicity results were reported for Pd^{II}·bleomycin and in pursuing a comparison with a cisplatin−bleomycin complex, we have performed cytotoxicity measurements in two leukemia cell lines using two methods. While complexation of bleomycin and cisplatin results in the decrease of their activity,[44] our data evidences that Pd^{II}·bleomycin exhibits comparable cytotoxicity with that of apo-bleomycin.

Results and Discussion

Interaction of Pd^{II} with Bleomycin

The first step in the structural characterization procedure of Pd^{II}·bleomycin was to prepare a pure and stable complex in aqueous media. Since Pd^{II} tends to undergo hydrolysis reactions,[45,46] addition of a twofold excess of K_2PdCl_4 in bleomycin solutions (1−10 mM concentrations) immediately produced a yellow, fine aggregate. Most likely, the insoluble product consists of hydroxo-bridged polynuclear Pd^{II} species. Even though mixing equimolar amounts of K_2PdCl_4 and bleomycin did not readily result in precipitation, a variety of compounds were formed, even at low pH (< 2). This was evident from the ^1H NMR spectra recorded immediately after mixing, which reveal the presence of at least three different species. Higher pH values and longer periods of time give rise to precipitation or formation of more complex mixtures.

Based on speciation studies of several Pd^{II} compounds analogous to cisplatin as a function of their concentration, pH and $[Cl^-]$,[47−50] we carried out the complex preparation in 1.0 M NaCl, so as to restrict the presence of aqua and/or hydroxo Pd^{II} species. As shown in Figure 1, under these

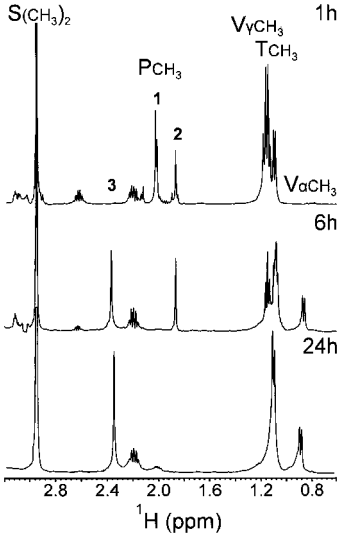

Figure 1. ^1H NMR spectral region of the Pd^{II}·bleomycin A2 system in 1.0 M NaCl at 298 K as a function of time; the resonances of the pyrimidine ring methyl protons ($P-CH_3$) reveal a three-step reaction and are indicated by the numbers 1, 2 and 3

conditions the ^{1}H NMR spectra indicate a multi-step reaction that occurrs during the first hours after mixing equimolar amounts of K_2PdCl_4 and bleomycin, which eventually leads to a major compound after 24 h at 40 °C. The complex formed is stable over a long period of several months, in neutral aqueous solutions (pH 6.7) of 10 mM concentration and at room temperature. This has allowed us to perform 2D NMR experiments and proceed to the structural determination of Pd^{II}·bleomycin A2.

Assignment and Analysis of the NMR Spectra

A strategy for the assignment of the non-exchangeable protons of bleomycin A2 has been previously presented in detail.[17,24] Combined use of heteronuclear and homonuclear experiments plays a key role in this procedure. A dispersion in the carbon dimension of the HMQC spectra (Figure S1 in the Supporting Information) in combination with the long-range couplings detected in the HMBC and TOCSY experiments have enabled us to assign the signals, especially the crowded disaccharide signals. ^{1}H and ^{13}C chemical shift values of Pd^{II}·bleomycin A2 are given in Tables S1 and S2 of the Supporting Information, in comparison with those reported for the metal-free bleomycin A2.[24,51]

Coordination of bleomycin to Pd^{II} through the pyrimidine and imidazole aromatic rings is readily detected by the changes in the **P**−CH_3 and **H**−C2H chemical shifts. In particular, the former signal appears at considerably lower field regions ($\Delta\delta$ = 0.4 ppm), which indicates a strong electron-withdrawing effect by the metal ion (see Figure 1). Despite the fact that both the ^{1}H and ^{13}C chemical shifts of the histidine **H**−Cα are not significantly affected upon complexation, the deprotonation of the histidine amide nitrogen is evident from the disappearance of its NH resonance. This is a strong indication for the coordination of the amide nitrogen to Pd^{II}, which was also the case for other metallo-bleomycins.[17,19,22−24,33−36] On the other hand, coordination of the β-aminoalanine secondary amine is reflected by the perturbation of the chemical shifts at **P**−CβH ($\Delta\delta$ = 0.4 ppm) and at the two **A**−$CβH_2$ ($\Delta\delta$ = 0.2−0.3 ppm).

Apart from the histidine amide proton, all the others were detected and assigned by observation of scalar couplings with their vicinal protons. Therefore, participation of any other amide nitrogen into the coordination sphere of Pd^{II}, rather than the deprotonated histidine amide, can be excluded. This is also true for the **V**−NH group (δ = 8.01), which has been proposed as a ligand for Pt^{II} and Pd^{II}·bleomycin.[44] The primary amine protons of β-aminoalanine exhibit a single resonance (δ = 6.39) strongly coupled to **A**−CαH. Their degeneration owning to the fast rotation around the C−N bond indicates that the primary amine is not coordinated, in contrast to Ga^{III} and In^{III}·bleomycins for which two strongly coupled signals had been detected.[22,23] Additionally, four pair of signals strongly coupled to each other were assigned to the pyrimidine ring **P**−NH_2 (δ = 7.51, 7.60), **P**−$CONH_2$ (δ = 7.08, 7.69), **A**−$CONH_2$ (δ = 6.93, 7.21) and **M**−$CONH_2$ (δ = 6.16, 6.61). The pyrimidine amine exhibits only medium-size NOEs with the neighbouring methyl group, in accordance with previous NMR studies.[17−19,22,23] **P**−$CONH_2$ and **A**−$CONH_2$ were assigned by virtue of their NOEs with the Cα and Cβ protons of the pyrimidinyl and aminoalanine moieties (see Figure 2). The remaining couple of fast exchanging protons was assigned to **M**−$CONH_2$, which did not show any cross-peak with other protons.

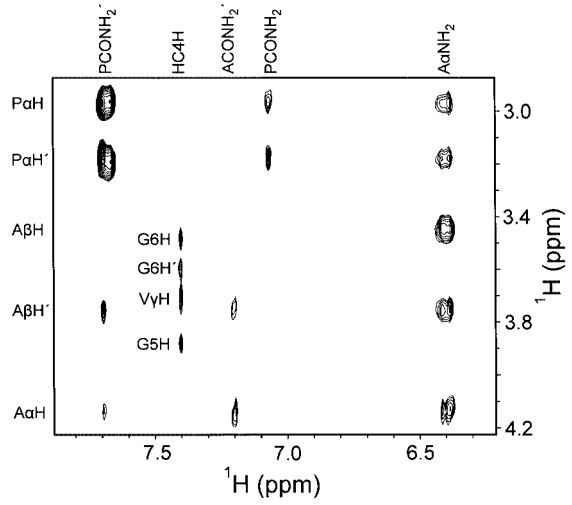

Figure 2. Expanded region from the NOESY spectrum of Pd^{II}·bleomycin A2 in H_2O (10% D_2O), 1.0 M NaCl, pH 6.7 at 278 K; the cross peaks shown are supporting the assignment of the exchangeable primary amine and amide protons

NOESY experiments were performed at 278 K and not only assisted in the assignment procedure, but also provided a wealth of structural information through distance constraints (Table S3 of the Supporting Information). Some common characteristics of metallo-bleomycins, such as the folding of the linker domain under the imidazole ring, were also exhibited by the Pd^{II}·bleomycin adduct. This is indicated by a number of NOEs between the aromatic protons of imidazole and the linker domain, especially by two medium intensity cross-peaks for **H**−C2H···**V**−CαH and **H**−C2H···**T**−CH_3. As a result of shielding by the imidazole ring current, **V**−CαH and **V**−αCH_3 proton signals appear at higher field compared with the metal-free bleomycin. Similarly, **M**−C3H is found to be shielded by the pyrimidine ring current, as the sugars move toward the metal-binding domain. In earlier NMR studies, the even higher upfield shift of the **M**−C3H signal ($\Delta\delta$ > 0.5 ppm) has been used as evidence for the coordination of the 3-*O*-carbamoyl nitrogen,[24] but it was disputed later.[17,19] Such stacking of the carbamoyl moiety over the pyrimidine ring has also been observed in the crystal structure of Cu^{II}·bleomycin A2.[16] Finally, the bithiazole and sulfonium

moieties of Pd^{II}·bleomycin lack any long-range NOEs with other domains, thus demonstrating a conformational flexibility.

Molecular Modelling and Structure Determination

Having established that the four common nitrogen ligands are involved in Pd^{II}·bleomycin and given that the square-planar geometry is the most favourable, three isomer models were constructed (see Scheme 2). To facilitate more extensive sampling of the conformational space, the disaccharide and β-aminoalanine moieties were placed at different orientations. In models I and II they were placed at opposite sides of the coordination plane, whereas in model III they both share the same side. Models I and II were based on the coordinates of the NMR structure of Co^{II}·bleomycin A2 (PDB code 1DEY),[41] while model III was based on the X-ray crystal structure of Cu^{II}·bleomycin A2 (PDB code 1JIF).[16]

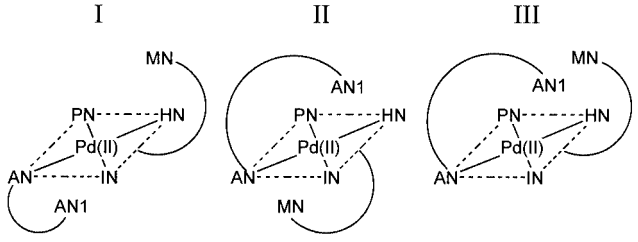

Scheme 2. Starting models employed in the molecular dynamics calculations; the ligands are designated as β-aminoalanine secondary amine (AN), pyrimidine N1 (PN), β-hydroxyhistidine amide (HN) and imidazole N1 (IN); the β-aminoalanine primary amine (AN1) and the mannose carbamoyl nitrogen (MN) occupy different sides of the equatorial plane in models I, II and the same side in model III

Each model was subjected to 20 runs of a simulated annealing calculation following the same protocol as that described for the structural determination of Ga^{III} and In^{III}·bleomycins.[22,23] After minimizing the energy of the initial models without any constraints, a molecular dynamics run was performed while increasing the temperature from 300 to 1000 K. The distance constraints were then gradually introduced and after allowing the system to overcome any potential energy minima, the temperature was decreased to 300 K. From the final 20 ps of the molecular dynamics run (at 300 K with distance constraints) 100 structures were collected and were superimposed by mass-weighted rms fittings of all heavy atoms excluding the bithiazole and C-terminal groups. Their coordinates were averaged and the final model was subjected to energy minimization until the rms gradient became less than 0.01.

The structural and energy statistics of the ten best structures for each model, by virtue of the lowest potential energy and lowest deviation from the restraints, are given in Table 1. Models I and III were found to be more consistent with the NMR constraints and they exhibited the lowest energy structures. Model II resulted in higher strain-energy structures in order to satisfy the restraints and can be readily excluded. Despite the different starting position of β-aminoalanine in models I and III, their final structures were quite similar. As a result, all structures of the isomers I and III exhibit minimal energy differences in comparison with those obtained by model II. Nevertheless, model III exhibits the most favourable results with minor restraint violations and the lowest total potential energy.

The solution structure of Pd^{II}·bleomycin A2 (see Figure 3) resulted by averaging the ten best structures of model III and by minimizing its strain energy. Selected structural data of the coordination plane are presented in Figure S2 (see Supporting Information). Some of the above-mentioned structural features of metallo-bleomycins were also identified in the Pd^{II} adduct. The linker domain of the two Co^{III}·bleomycin complexes is folded under the equatorial plane from the side of the imidazole. The basis of this folding has been related to the interaction of the hydroperoxide or hydroxide axial ligand with the linker backbone.[17,19] In our case, a similar folding of the linker domain can be attri-

Table 1. Structural and energy statistics for the three Pd^{II}·bleomycin A2 models, which were obtained from the simulated annealing molecular dynamics calculations; for each model, ten structures were obtained by mass-weighted rms fitting and averaging the coordinates from the last 20 ps of the trajectory (100 snapshots); statistics were obtained after energy minimization was performed with all the distance restraints applied

	Model I	Model II	Model III
Rmsd. of heavy atoms[a] (Å)	0.77 ± 0.35	1.55 ± 0.44	0.11 ± 0.03
Distance restraint violations > 0.01 Å	7−13	12−16	4−9
Rmsd. from distance restraints (Å)	0.035 ± 0.012	0.040 ± 0.008	0.024 ± 0.004
Potential energy terms: (kcal mol^{-1})	−4.7 ± 4.8	24.6 ± 7.7	−10.4 ± 6.3
Total	13.9 ± 0.4	15.0 ± 1.1	14.6 ± 0.3
Bond	66.1 ± 3.1	71.1 ± 3.2	62.4 ± 1.1
Angle	48.2 ± 2.9	53.6 ± 4.6	44.7 ± 2.6
Dihedral angle[b]	−138.2 ± 6.2	−121.2 ± 7.6	−134.7 ± 7.0
Non-bonded constraint[c]	5.3 ± 3.3	6.1 ± 2.6	2.6 ± 0.7

[a] The atoms of bithiazole and sulfonium moieties were not included due to the disorder of this domain. [b] Including also an improper angle-energy term. [c] The sum of the electrostatic and van der Waals energy terms.

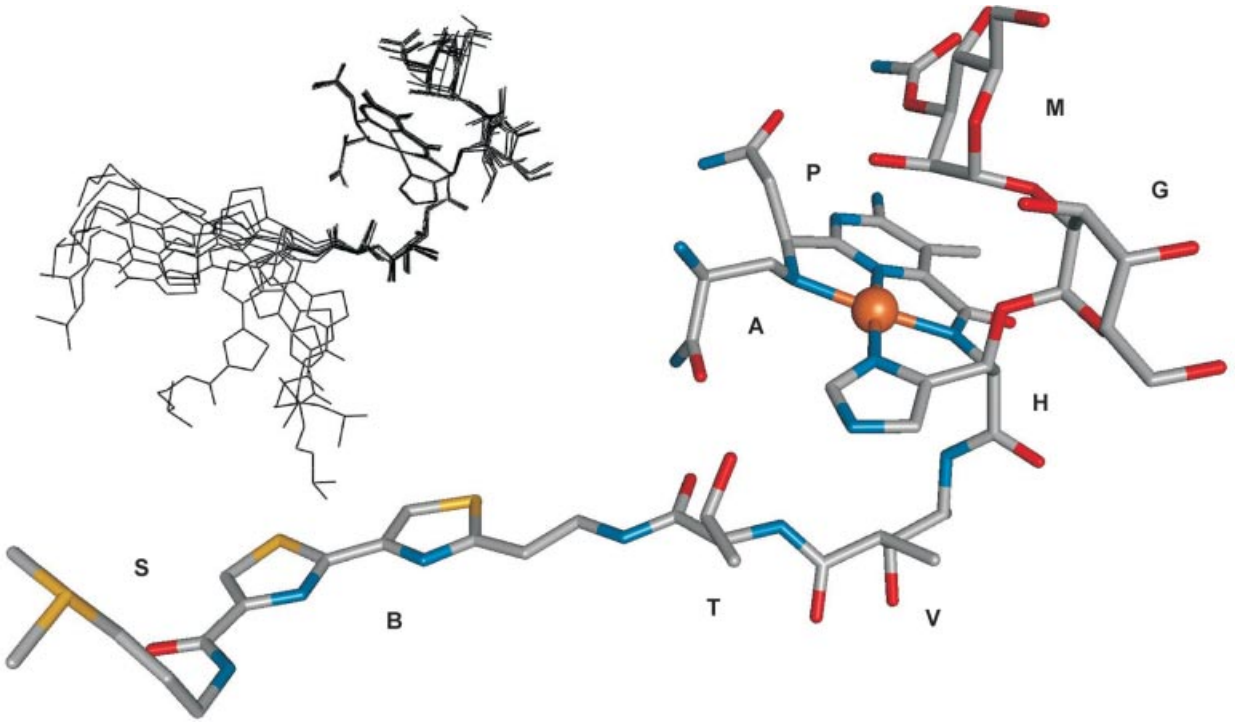

Figure 3. Structure of Pd^{II}·bleomycin A2 calculated from the averaged coordinates of the ten best models of III (shown in the inset) after energy minimization with all the constraints applied; atom colours are grey for C, blue for N, red for O, yellow for S and orange for Pd

buted to the H bonds, which were exhibited between the threonine and aminoalanine moieties (**T**−O−H···O=C−**A** and **T**−C=O···H−N−**A**). Their geometric characteristics indicate a strong interaction, which can account for the folding observed (Figures S3 and S4 in the Supporting Information). This interaction is supported by the strong chemical shift perturbation of **A**−$CONH_2$ protons (Table S1) and by a medium and a weak NOE between the two **A**−$CONH_2$ protons and **T**−NH (Table S3).

The disaccharide moiety of bleomycin is found to be positioned over the plane, which can be due to an additional H bond between the propionamide and carbamoyl moieties (**P**−C=O···H−N−**M**). But since the **P**−$CONH_2$ and **M**−$CONH_2$ signals are marginally perturbed upon complexation (Table S1 in Supporting Information) this interaction cannot be explicitly defined. In addition, it is also possible that water molecules mediate H-bonding interactions between mannose and propionamide domains, an interaction that cannot be simulated without explicit treatment of the solvent. As shown in Figure 3, the aminoalanine moiety is located away from the metal ion. If **A**−αNH_2 occupied the initial position over the metal, then it would be expected to participate in an axial Pd···H−N interaction. This would contradict our NMR spectroscopic data, since one of the degenerate resonances from the interacting amine proton should be shifted to lower field. Indeed, examination of the final model revealed that axial Pd···H−X (X = calcd. C, O, N) interactions are absent. Finally, the thiazolium rings are shown in the *cis* conformation, by virtue of a quite weak NOE detected between their two aromatic protons (not used as distance constraint).

Antitumor Activity

The cytotoxicity of the Pd^{II}·bleomycin A2 complex was screened in two leukemia cell lines, human chronic myeloid leukemia (K562) and human histiocytic lymphoma (U937). K562 cells were incubated with higher concentrations of the drugs (100 and 300 μg/ml) than U937 cells (10 and 100 μg/ml), since the former are less sensitive to several anticancer agents. Incubation times were 6 to 48 hours. Two different methods were used, in order to assess the percentage of total alive cells (MTT) and the number of necrotic cells (Trypan Blue). The MTT assay is based on an enzymatic reaction and is therefore more sensitive and accurate. Since MTT is absorbed by the mitochondria, it is transformed into formazan by the enzyme succinic dehydrogenase. By assessing the activity of the mitochondrial dehydrogenases, the activity of viable cells is screened. The results obtained by both methods are presented in Table S4 (see Supporting Information).

The results obtained using the MTT assay, which are illustrated in Figure 4, show that the cytotoxicity exhibited by Pd^{II}·bleomycin is similar to that of the free drug. For both cell lines, the toxicity of the complex was measured as being 10 % lower than that of bleomycin, following the same trend as a function of time. A plausible explanation for the toxicity demonstrated by Pd^{II}·bleomycin is that the complex dissociates under cellular conditions. By virtue of its lack of redox activity and inability to mediate DNA-strand scission, the cytotoxicity is most probably due to the free drug released into the cells. Based on this hypothesis, the percentage of lower toxicity of Pd^{II}·bleomycin can be

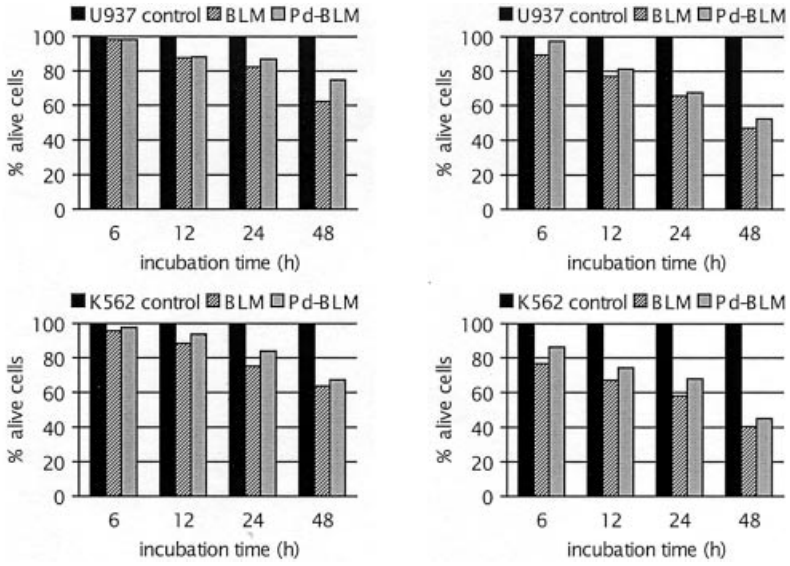

Figure 4. Antitumor activity of the Pd^{II}·bleomycin A2 complex (Pd-BLM) in comparison with that exhibited by the metal-free drug (BLM) as a function of time; the upper diagrams illustrate the results obtained by the MTT assay for U937 cells, after incubation with 10 μg/ml (left) and 100 μg/ml (right) of drugs; the lower diagrams were obtained by the same method as for K562 cells, after incubation with 100 μg/ml (left) and 300 μg/ml (right) of drugs

attributed to the presence of an equilibrium between the metal-bound and the apo-form of bleomycin. It is possible that the stability of the complex observed does not correspond to the same stability under cellular conditions, which are quite different to those of the NMR experiments.

In order to obtain more information on the stability of the complex, we performed NMR and circular dichroism (CD) studies on Pd^{II}·bleomycin in lower salt concentrations. For this reason we diluted a stock 10 mM solution of the complex (1.0 M NaCl, pH = 6.7) in H_2O, so that the final salt concentration was 4−150 mM, while the drug concentration was 0.04−1.5 mM. The pH was adjusted to 7.2 using aliquots from dilute NaOH and the solutions were incubated at 37 °C. All spectra were recorded at room temperature starting one hour after each dilution and lasting up to three days. Seeing that no changes occur either in the CD spectra (solutions with [drug] < 0.5 mM), or the NMR spectra (solutions with [drug] > 0.5 mM), we cannot support the hypothesis that Pd^{II}·bleomycin dissociates under cellular conditions.

On the other hand, we cannot rule out the possibility that Pd^{II}·bleomycin mediates the cytotoxicity observed, without requiring the redox activation of oxygen. Based on observations in vitro that the complex is not only able to bind strongly to DNA, but it can also displace Fe^{III} from its coordination site,[44] the cytotoxicity of Pd^{II}·bleomycin could be attributed to its DNA-binding ability or any other mechanism that may lead to the cell death (such as apoptosis). But taking into consideration that Pt^{II}·bleomycin exhibits a strong affinity for DNA and that the complexation of bleomycin and cisplatin gives rise to a decrease in the cytotoxicity of both drugs,[44] albeit screened in different cell lines, the hypothesis that Pd^{II}·bleomycin dissociates under cellular conditions seems more plausible. Still, further investigations should be carried out, in order to elucidate the mechanism of cytotoxicity. A related paradigm is the case of Cu·bleomycin, which was initially considered as an inhibitor of DNA cleavage.[52] However, later findings have suggested that it may assist in generating an active Fe·bleomycin species in vivo, a mechanism that still remains a puzzle.[12]

Conclusion

Following the procedure described herein, we prepared the Pd^{II}·bleomycin A2 complex in aqueous media and determined its solution structure using NMR spectroscopy in combination with molecular dynamics calculations. Our data reveal that bleomycin binds to Pd^{II} adopting a conformation similar to most of the models proposed either by NMR or X-ray crystallography. The same N ligands involved in the equatorial planes of Cu^{II}, Fe^{II}, Co^{II} and Co^{III}, Ga^{III} and In^{III} metallo-bleomycins are shown to be arranged in a square-planar geometry around Pd^{II}. Cytotoxicity measurements in two leukemia cell lines demonstrate that Pd^{II}·bleomycin is almost as toxic as the free drug, in contrast to Pt^{II}·bleomycin, which was found to have lower toxicity than apo-bleomycin.

Experimental Section

Sample Preparation: Bleocin and pure bleomycin A2 sulfate were a kind offer from Nippon Kayaku Co. Ltd. and were used without further purification. The complex was prepared by mixing equimolar amounts of K_2PdCl_4 (100 mM) and bleomycin (10 mM) in aqueous solutions containing NaCl (1.0 M). The pH of the solution, which immediately dropped below 2.0, was slowly increased to 3.5 using aliquots of dilute NaOH (1.0 M). After heating the mixture at 40 °C for 2 h, its pH, which continuously dropped, was then

increased to 5.0. This procedure was repeated twice before the pH was finally increased to 7.0. The mixture was then heated at 40 °C for 24 h, so as to assure complete formation of the complex and the pH was finally readjusted to 6.7. Its stability over a period of several months at room temperature is demonstrated by the fact that no changes were detected in the ^{1}H NMR spectra. Using the same procedure, Pd^{II}·bleomycin was also prepared in Millipore water for the cytotoxicity measurements.

NMR Experiments: Samples for the NMR experiments were prepared either in H_2O (10% D_2O) or D_2O 99.99%. All spectra were recorded on a Bruker Avance NMR spectrometer operating at proton frequency of 500.13 MHz. X-WIN NMR 2.6 (Bruker Analytik GmbH) was used to process the spectra and SPARKY 3.1,[53] running on a Linux PC, was used for the assignment and analysis of the 2D spectra. ^{1}H and ^{13}C chemical shift values were referenced to an internal standard, sodium 3-(trimethylsilyl)-1-propanesulfonate (TSP).

Two-dimensional NOESY (100, 200 and 400 ms mixing times), DQF COSY,[54] and TOCSY (MLEV-17 sequence with 35 and 70 ms mixing times)[55] experiments were performed at 278 and 298 K in H_2O and D_2O. Data sets with 2048 × 512 complex points were acquired with 7 KHz-sweep widths in both dimensions and 32 scans per t_1 increment. ^{1}H{^{13}C} HMQC[56] and HMBC[57] spectra were recorded at 278 and 298 K in H_2O and D_2O. Data sets with 1024 × 256 points were collected with 32 or 64 scans per t_1 increment and spectral widths of 6 KHz in the proton and 25 kHz in the carbon dimension. Solvent suppression for the H_2O samples was performed using excitation sculpting with gradients,[58] while for the D_2O samples a pre-saturation pulse was applied during the relaxation delay of 2.0 s. The indirect dimension was zero-filled up to 1024 data points and the FIDs were processed with either a combination of exponential and Gaussian weighting functions or a 90°-shifted sine-bell function.

Force Field Parameters: All molecular modelling calculations were performed with AMBER 6.[59] In order to accurately represent the bleomycin complex, the AMBER-94 force field was modified according to the guidelines of its authors.[60] Standard atom types were assigned to the atoms of bleomycin by analogy with their chemical environment. For the sugar atoms, we used parameters from the GLYCAM force field for modelling carbohydrates.[61] A new atom type was created for Pd^{II} using the van der Waals parameters R^* = 1.65 Å and ε = 0.20 kcal mol^{-1}, based on the crystallographic data of Bondi.[62] According to the calculations of Hambley,[63] these parameters reproduce quite well the metal−ligand separations in molecular mechanics force fields. The bond, angle and dihedral angle parameters of bleomycin were also chosen upon their analogy with existing parameters of AMBER, while those involving Pd^{II} were adapted from parameters developed for platinum compounds.[64] Equilibrium Pd−N bond lengths were set to R_o of 2.01 Å using a relatively low force constant of 100 kcal mol^{-1} Å^{-2}. For the N−Pd−N angles, θ_o of 90° or 180° with 40 kcal mol^{-1} rad^{-2} force constants were used, while dihedral angles involving the metal were set with zero force constants.

The atom-centred point charges of the complex were generated from the electrostatic potential of its molecular fragments. The equatorial plane of Pd^{II}·bleomycin comprising β-aminoalanine, pyrimidinyl propionamide and histidyl moieties was fitted as a whole. For the other domains we used the charges, which had been previously calculated for Ga^{III}·bleomycin.[22] Spin-restricted DFT calculations using Becke's three-parameter-hybrid functional with the correlation functional of Lee, Yang, and Parr (B3LYP)[65−67] were performed using the program package GAMESS.[68] The Los Alamos effective core potentials were applied on palladium,[69−71] and the 6−31G(d) basis set on all other atoms. The point charges were fitted to reproduce the electrostatic potential using the RESP method,[72] a two-stage approach where the equivalent methyl and methylene hydrogen atoms are restrained to have the same charge. In order to reassemble the charges of the entire molecule, the H-neutralization method was used.[73]

Restrained Molecular Dynamics: NOE signals from the NOESY spectrum (200 ms mixing time at 278 K, pH 6.7) were classified as strong, medium and weak by visual inspection of the cross-peak intensities and the constraints were set to an upper distance limit of 3.0, 4.0 and 5.0 Å, respectively. An additional 1.0 Å was allowed for NOEs involving methyl groups and ambiguous methylene protons. A total of 76 distance constraints were applied with a 50 kcal mol^{-1} Å^{-2} force constant, using a square-bottom-well function with parabolic sides out to 0.5 Å and then linear sides beyond that. Molecular dynamics calculations in vacuo were carried out at a time step of 1 fs with the distance-dependent dielectric constant algorithm of AMBER. The cut-off distance was set to 16.0 Å and the non-bonded pair list was updated every ten steps. Temperature regulation was performed using the Berendsen algorithm. For the heating and cooling stages, a bath coupling constant of 0.1−0.5 ps was applied, in order to assure a tighter coupling to the heat bath, while for the equilibration stages it was increased up to 2.0 ps, so as to allow sampling of more natural trajectories. Starting models were energy minimized prior to the simulated annealing calculations without restraints for 500 steps of the steepest descent method, followed by the conjugate gradient method until the rms gradient became less than 0.1.

Each model was subjected to 20 individual runs, while changing the initial velocities assigned. The annealing protocol consisted of five stages: (1) heating the system from 5 K up to 1000 K during the first 20 ps, (2) gradual application of the constraints for a period of 10 ps, (3) high-temperature equilibration for 20 ps, (4) slow cooling down to 300 K during the next 20 ps and (5) final dynamics run for 50 ps at 300 K. A final model from each iteration was generated by mass-weighted rms fitting and averaging the coordinates from the last 20 ps of the trajectory (100 structures). Energy minimization with restraints was performed as above but until the rms gradient became less than 0.01. The results presented in Table 1 were derived from the ten best structures, which were favoured by their low potential energy and minimal deviations from the NMR constraints.

Cell Lines and Cytotoxicity Assays: RPMI 1640, Fetal Bovine Serum (FBS), penicillin, streptomycin, Phosphate Buffered Saline (PBS) and HEPES buffer were purchased from BIOCHROM. L-Glutamine was purchased from AppliChem. Trypan Blue, 3-(4,5-dimethylthiazol-2-yl)-2,5-diphenyl-tetrazolium bromide (MTT), sodium dodecyl sulfate (SDS), formamide and $NaHCO_3$ were purchased from Sigma−Aldrich. Two human cell lines routinely maintained in the Biology department of NCSR "Demokritos" were used in this study. Chronic myelogenic leukemia (K562) and human promyelocytic cell line (U937) were maintained in RPMI 1640 medium containing 10% (v/v) FBS, 2 mM L-glutamine, 0.85 g/l $NaHCO_3$, 25 mM HEPES, 200 U/ml penicillin and 100 μg/ml streptomycin at 37 C in a 5% CO_2 atmosphere. The pH of the medium was adjusted to 7.3. In all experiments, cells were cultured to the logarithmic phase growth over a period of 48 h, starting from a culture density of 3−5 × 10^5 cells/ml.

The viability of the cells was determined by the Trypan Blue dye-exclusion method and cytotoxicity was assessed by the MTT assay.[74−77] Briefly, logarithmically grown cells were plated in 25-

mL flasks and treated with two concentrations of each drug. Untreated cells were used as a negative control. Incubation was carried out at 37 °C for different time periods, starting from a 6 h incubation up to 50 h. After drug incubation for various time periods at 37 °C, MTT (50 µl, 10 mg/ml) was added to each well, followed by a 4 h incubation at 37 C. The reaction results in the reduction of MTT by the mitochondrial dehydrogenases of viable cells to a purple formazan product. Cells were lysed using DMF solution (55 mL H_2O + 12.5 g SDS + 45 mL formamide, pH 4.7) and left overnight at 37 °C. After centrifugation, 200 µL of each sample were placed in 96-well microtiter plates in duplicate and $OD_{550\ nm}$ was determined in an ELISA plate reader. The results are expressed as the percentage of alive cells, calculated from MTT reduction and it is assumed that the absorbance of control cells is 100%. In addition, cell viability in U937 and K562 cell lines was assessed by the method of Trypan Blue exclusion. Trypan blue (0.2%, 2 µl) was added to aliquots of cell-containing media (18 µl) and the percentage of viable cells was determined by counting the number of cells able to exclude the dye on an hemocytometer. All of the above experiments were performed in duplicate.

Supporting Information (see also the footnote on the first page of this article): Two tables giving the ^1H and ^{13}C chemical shift values of Pd^{II}·bleomycin A2 in comparison with those obtained for the metal-free bleomycin A2, a table with the categorized NOE intensities, a table with all the results from the cytotoxicity measurements, a figure showing an expanded region of the $^1H\{^{13}C\}$ HMQC spectrum and three figures illustrating the solution structure of Pd^{II}·bleomycin A2 along with selected structural data of the coordination sphere, potential intramolecular H-bonds and a comparison with the crystal structure of Cu^{II}·bleomycin.

Acknowledgments

We are grateful to Prof. Ivano Bertini for his hospitality at the University of Florence (CERM) in the framework of the European Large Scale Research Infrastructure. We thank Prof. Enzo Alessio for his critical comments on the manuscript. This work has been supported with a grant by the General Secretariat for Research and Technology of Greece.

[1] H. Umezawa in *Anticancer Agents Based on Natural Product Models* (Eds: J. M. Cassady, J. Douros), Academic Press, New York, **1980**, pp. 147−166.
[2] B. I. Sikic, M. Rosencweig, S. K. Carter, *Bleomycin Chemotherapy*, Academic Press, Orlando, **1985**.
[3] J. S. Lazo, B. A. Chabner in *Cancer Chemotherapy and Biotherapy: Principals and Practice* (Eds.: B. A. Chabner, D. L. Longo), 2nd ed., Lippincott−Raven, Philadelphia, PA, **1996**, p. 379.
[4] S. M. Hecht, *Acc. Chem. Res.* **1986**, *19*, 383−391.
[5] J. Stubbe, J. W. Kozarich, *Chem. Rev.* **1987**, *87*, 1107−1136.
[6] M. J. Absalon, W. Wu, J. W. Kozarich, J. Stubbe, *Biochemistry* **1995**, *34*, 2076−2086.
[7] J. Stubbe, J. W. Kozarich, W. Wu, D. E. Vanderwall, *Acc. Chem. Res.* **1996**, *29*, 322−330.
[8] D. L. Boger, H. Cai, *Angew. Chem.* **1999**, *111*, 470−500; D. L. Boger, H. Cai, *Angew. Chem. Int. Ed.* **1999**, *38*, 448−476.
[9] R. M. Burger, *Chem. Rev.* **1998**, *98*, 1153−1169.
[10] K. E. Loeb, J. M. Zaleski, C. D. Hess, S. M. Hecht, E. I. Solomon, *J. Am. Chem. Soc.* **1998**, *120*, 1249−1259.
[11] N. Lehnert, F. Neese, R. Y. N. Ho, L. Que Jr., E. I. Solomon, *J. Am. Chem. Soc.* **2002**, *124*, 10810−10822.
[12] C. A. Claussen, E. C. Long, *Chem. Rev.* **1999**, *99*, 2797−2816.
[13] H. Umezawa, K. Maeda, T. Takeuchi, Y. Okami, *J. Antibiot.* **1966**, *19*, 200−209.
[14] Y. Iitaka, H. Nakamura, T. Nakatani, Y. Muraoka, A. Fujii, T. Takita, H. Umezawa, *J. Antibiot.* **1978**, *31*, 1070−1072.
[15] T. Takita, Y. Muraoka, T. Nakatani, A. Fujii, Y. Iitaka, H. Umezawa, *J. Antibiot.* **1978**, *31*, 1073−1077.
[16] M. Sugiyama, T. Kumagai, M. Hayashida, M. Maruyama, *Biol. Chem.* **2002**, *277*, 2311−2320.
[17] W. Wu, D. E. Vanderwall, J. W. Kozarich, J. Stubbe, C. J. Turner, *J. Am. Chem. Soc.* **1994**, *116*, 10843−10844.
[18] W. Wu, D. E. Vanderwall, S. M. Lui, X.-J. Tang, C. J. Turner, J. W. Kozarich, J. Stubbe, *J. Am. Chem. Soc.* **1996**, *118*, 1268−1280.
[19] S. M. Lui, D. E. Vanderwall, W. Wu, X.-J. Tang, C. J. Turner, J. W. Kozarich, J. Stubbe, *J. Am. Chem. Soc.* **1997**, *119*, 9603−9613.
[20] D. E. Vanderwall, S. M. Lui, W. Wu, C. J. Turner, J. W. Kozarich, J. Stubbe, *Chem. Biol.* **1997**, *4*, 373−387.
[21] S. T. Hoehn, H.-D. Junker, R. C. Bunt, C. J. Turner, J. Stubbe, *Biochemistry* **2001**, *40*, 5894−5905.
[22] A. Papakyriakou, B. Mouzopoulou, N. Katsaros, *J. Biol. Inorg. Chem.* **2003**, *5*, 549−559.
[23] A. Papakyriakou, N. Katsaros, *Eur. J. Inorg. Chem.* **2003**, *16*, 3001−3006.
[24] M. A. J. Akkerman, E. W. J. F. Neijman, S. S. Wijmenga, C. W. Hilbers, W. Bermel, *J. Am. Chem. Soc.* **1990**, *112*, 7462−7474.
[25] T. E. Lehmann, L.-J. Ming, M. E. Rosen, L. Que Jr., *Biochemistry* **1997**, *36*, 2807−2816.
[26] R. P. Sheridan, R. K. Gupta, *J. Biol. Chem.* **1981**, *256*, 1242−1247.
[27] G. M. Ehrenfeld, N. Murugesan, S. M. Hecht, *Inorg. Chem.* **1984**, *23*, 1496−1498.
[28] R. M. Burger, J. Peisach, *J. Inorg. Chem.* **1984**, *23*, 2215−2217.
[29] H. B. Grey, R. Margalit, J. M. Clarke, L. Podbielski, *Chem. Biol. Interact.* **1986**, *59*, 231−245.
[30] B. Mouzopoulou, H. Kozlowski, N. Katsaros, A. Garnier-Suillerot, *Inorg. Chem.* **2002**, *40*, 6923−6929.
[31] L. Banci, A. Dei, D. Gatteschi, *Inorg. Chim. Acta* **1982**, *67*, L53−L55.
[32] J. Kuwahara, T. Suzuki, Y. Sugiura, *Biochem. Biophys. Res. Commun.* **1985**, *129*, 368−374.
[33] M. A. J. Akkerman, C. A. G. Haasnoot, C. W. Hilbers, *Eur. J. Biochem.* **1988**, *173*, 211−225.
[34] R. A. Manderville, J. F. Ellena, S. M. Hecht, *J. Am. Chem. Soc.* **1994**, *116*, 10851−10852.
[35] R. A. Manderville, J. F. Ellena, S. M. Hecht, *J. Am. Chem. Soc.* **1995**, *117*, 7891−7903.0.
[36] A. M. Calafat, H. Won, L. G. Marzilli, *J. Am. Chem. Soc.* **1997**, *119*, 3656−3664.
[37] J. D. Otvos, W. E. Antholine, S. Wehrli, D. H. Petering, *Biochemistry* **1996**, *35*, 1458−1465.
[38] A. Dei, D. Gatteschi, *J. Inorg. Biochem.* **1982**, *17*, 131−137.
[39] L. L. Guan, J. Kuwahara, Y. Sugiura, *Biochemistry* **1993**, *32*, 6141−6145.
[40] R. E. Lenkinski, B. E. Peerce, R. P. Pillai, J. D. Glickson, *J. Am. Chem. Soc.* **1980**, *102*, 7088−7093.
[41] T. E. Lehmann, M. L. Serrano, L. Que Jr., *Biochemistry* **2000**, *39*, 3886−3898.
[42] T. E. Lehmann, *J. Biol. Inorg. Chem.* **2002**, *7*, 305−312.
[43] G. J. Bosl, D. F. Bajorin, J. Sheinfeld in *Cancer: Principles and Practice of Oncology* (Eds.: V. T. DeVita, S. Hellman, S. A. Rosenberg), 6th ed., Lippincott Williams & Wilkins, Philadelphia, PA, **2001**, pp. 1491−1518.
[44] J. P. Albertini, A. Garnier-Suillerot, *Inorg. Chem.* **1986**, *25*, 1216−1221.
[45] R. B. Martin in *Platinum, Gold and Other Metal Chemotherapeutic Agents* (Ed.: S. J. Lippard), ACS Symposium Series 209, American Chemical Society, Washington, DC, **1983**, pp. 231−244.

[46] M. Kotowski, R. van Eldik, *Inorg. Chem.* **1984**, *23*, 3310−3312.
[47] H. Hohmann, R. van Eldik, *Inorg. Chim. Acta* **1990**, *174*, 87−92.
[48] T. G. Appleton, A. J. Bailey, D. R. Bedgood, J. R. Hall, *Inorg. Chem.* **1994**, *33*, 217−226.
[49] J. M. Tercero-Moreno, A. Matilla-Hernández, S. González-García, J. Niclós-Gutiérrez, *Inorg. Chim. Acta* **1996**, *253*, 23−29.
[50] M. L. González, J. M. Tercero, A. Matilla, J. Niclós-Gutiérrez, M. T. Fernández, M. C. López, S. González, *Inorg. Chem.* **1997**, *36*, 1806−1812.
[51] C. Xia, F. H. Försterling, D. H. Petering, *Biochemistry* **2003**, *42*, 6559−6564.
[52] E. A. Sausville, J. Peisach, S. B. Horwitz, *Biochemistry* **1978**, *17*, 2740−2746.
[53] T. D. Goddard, D. G. Kneller, *SPARKY 3*, University of California, San Francisco, **2002**.
[54] A. Derome, M. Williamson, *J. Magn. Reson.* **1990**, *88*, 177−185.
[55] A. Bax, D. G. Davis, *J. Magn. Reson.* **1985**, *65*, 355−360.
[56] A. Bax, S. Subramanian, *J. Magn. Reson.* **1986**, *67*, 565−569.
[57] A. Bax, M. F. Summers, *J. Am. Chem. Soc.* **1986**, *108*, 2093−2094.
[58] T. L. Hwang, A. J. Shaka, *J. Magn. Reson.* **1995**, *112*, 275−279.
[59] D. A. Case, D. A. Pearlman, J. W. Caldwell, T. E. Cheatham, W. S. Ross, C. L. Simmerling, T. A. Darden, K. M. Merz, R. V. Stanton, A. L. Cheng, J. J. Vincent, M. Crowley, V. Tsui, R. J. Radmer, Y. Duan, J. Pitera, I. Massova, G. L. Seibel, U. C. Singh, P. K. Weiner, P. A. Kollman, *AMBER 6*, University of California, San Francisco, **1999**.
[60] W. D. Cornell, P. Cieplak, C. I. Bayly, I. R. Gould, K. M. Merz Jr., D. M. Ferguson, D. C. Spellmeyer, T. Fox, J. W. Caldwell, P. A. Kollman, *J. Am. Chem. Soc.* **1995**, *117*, 5179−5197.
[61] R. J. Woods, R. A. Dwek, C. J. Edge, B. Fraser-Reid, *J. Phys. Chem.* **1995**, *99*, 3832−3846.
[62] A. Bondi, *J. Phys. Chem.* **1964**, *68*, 441−451.
[63] T. W. Hambley, *Inorg. Chem.* **1998**, *37*, 3767−3774.
[64] T. W. Hambley, A. R. Jones, *Coord. Chem. Rev.* **2001**, *212*, 35−59.
[65] A. D. Becke, *Phys. Rev. A.* **1988**, *38*, 3098−3100.
[66] A. D. Becke, *J. Chem. Phys.* **1993**, *98*, 1372.
[67] A. D. Becke, *J. Chem. Phys.* **1993**, *98*, 5648−5652.
[68] M. W. Schmidt, K. K. Baldridge, J. A. Boatz, S. T. Elbert, M. S. Gordon, J. J. Jensen, S. Koseki, N. Matsunaga, K. A. Nguyen, S. Su, T. L. Windus, M. Dupuis, J. A. Montgomery, *J. Comput. Chem.* **1993**, *14*, 1347−1363.
[69] P. J. Hay, W. R. Wadt, *J. Chem. Phys.* **1985**, *82*, 270−283.
[70] P. J. Hay, W. R. Wadt, *J. Chem. Phys.* **1985**, *82*, 299−310.
[71] W. R. Wadt, P. J. Hay, *J. Chem. Phys.* **1985**, *82*, 284−298.
[72] C. I. Bayly, P. Cieplak, W. D. Cornell, P. A. Kollman, *J. Phys. Chem.* **1993**, *97*, 10269−10280.
[73] L. Young, I. A. Topol, A. A. Rashin, S. K. Burt, *J. Comput. Chem.* **1997**, *18*, 522−532.
[74] T. Mosmann, *J. Immunol. Methods* **1983**, *65*, 55−63.
[75] H. Tada, O. Shino, K. Kurosima, M. Koyama, K. Tsukamoto, *J. Immunol. Methods* **1986**, *93* 157−165.
[76] M. B. Hansen, S. E. Nielsen, K. Berg, *J. Immunol. Methods* **1989**, *119*, 203−210.
[77] M. B. Hansen, C. Ross, K. Berg, *J. Immunol. Methods* **1990**, *127*, 241−248.

Received January 15, 2004
Early View Article
Published Online May 25, 2004

